19th IMEKO TC10 Conference
"MACRO meets NANO in Measurement for Diagnostics, Optimization and Control"
Delft, The Netherlands, September 21–22, 2023

The Detection of Rotor Bar Faults in Induction Motors Using the Recursive Matrix Pencil Method

Alexander Shestakov, Olga Ibryaeva, Victoria Eremeeva, Vladimir Sinitsin

South Ural State University, Chelyabinsk, Russia, ibriaevaol@susu.ru

Abstract – Rotor cage induction motors are widely used in the industry and their unpredicted shutdown can be very costly. Therefore, for safety and economic considerations, there is a need for identifying incipient faults. Among the induction motors faults, the rotor bar faults are among the most common failures. These generate sideband frequency components around the frequency of the power supply. The amplitudes of these sideband frequencies increase with the progression of the bar fault. Here we propose that the Recursive Matrix Pencil Method is able to track the growth of the sideband frequency amplitude excited by a rotor bar fault and show the results of applying the technique to numerically simulated data. Signal preprocessing consists in filtering the supply frequency and bandpass filtering with a passband frequency range specified by one of the sideband frequencies. The paper uses the modelling of the induction motor current signal so that the gradual development of a rotor bar fault can be simulated. It is shown that the Recursive Matrix Pencil Method gives a time advantage over the Classical Matrix Pencil Method and the possibility of practical application.

Keywords – Matrix Pencil Method, Induction Motor, Rotor Bar Faults, Diagnostic, Current Signal Analysis

I. INTRODUCTION

Rotor cage induction motors are the most common type of electric machines used in the engineering, metallurgical, mining, and aviation industries [1] due to their operation performance and low maintenance costs.

Heavy industries have harsh operating conditions, which often lead to motor component wear—up to 15% of industrial motors fail annually [2]. Even if wear does not cause the motor to fail, efficiency may be compromised. The operation of a defective motor is accompanied by torque and speed fluctuations and additional vibrations. In this case, the efficiency of the motor drops by 3 % to 13 %, which leads to an increase in power consumption [3].

Approximately 10 % of induction motor faults occur in the rotor [4], where broken rotor bars or cracked end rings are the most common issues. The challenges of diagnostics are the weak fault signatures which are difficult to detect with simple methods. Furthermore, rotor axial air ducts, low frequency load oscillations, and rotor core anisotropy may cause false alarms, which can be misinterpreted as induction-motor rotor faults [5]. Therefore, the industry increasingly needs more efficient methods and tools to diagnose and assess induction motor health status.

Motor Current Signature Analysis (MCSA) is one of the most extensively utilized technique for rotor bar diagnostics. It detects, from current signals, the specific signature associated with a fault. One of the major difficulties for detecting bar fault-related harmonics in MCSA is the fundamental frequency harmonic, which is considered as "noise" from the point of view of fault detection.

The MUSIC and ESPRIT methods can find the defect harmonics in noise under non-stationary conditions, but have high computational complexity. The Prony method has lower computational costs, but its efficiency decreases sharply with increasing noise level in the signal [6]. The Matrix Pencil Method (MPM) is a development of the Prony method. The computational efficiency of MPM is 5.7 times higher than that of MUSIC and ESPRIT [7]. The MPM was used in the diagnosis of broken rotor bars [7-9]. Thus, in [7], the authors combined the classical MPM with a classifier based on the support vector machine algorithm. In [8], an adaptive MPM with auto-tuning of the response threshold based on information entropy was proposed. This method can accurately detect symptoms of mixed rotor faults at low load and low motor speed in steady state. In [9], the MPM and Wiener filter are applied to the current signals of a motor with a rotor defect to remove known signal harmonics and improve the signal-to-noise ratio. Thus, the MPM has the potential to effectively detect motor rotor defect symptoms under unsteady conditions.

This paper proposes a new technique in the diagnostics of rotor bar faults based on the Recursive Matrix Pencil Method (RMPM). The method works in a moving window manner and tracks the value of the amplitude of a fault characteristic frequency, which grows with the development of this defect. In the proposed technique, the

signal undergoes a preliminary filtering of the supply frequency and bandpass filtering with a passband frequency range specified by one of the sideband frequencies.

The paper is organized as follows. Section 2 describes the signal model used. Note that this paper models induction motor current signal so that the gradual development of a bar fault can be simulated, which is difficult to do experimentally. The processing technique based on RMPM is presented in Section 3. The method uses the procedure for filtering known components described in Section 4. The numerical simulated current signal with an incipient bar fault is considered for the validation of the proposed method in Section 5.

The main contribution of this article is that RMPM can be used as a diagnostic tool in rotor bar fault detection, tracking the amplitude of a sideband frequency. The methodology was validated by using simulation signals, and its effectiveness is presented.

II. MOTOR CURRENT SIMULATION SIGNAL

In this paper, a mathematical model based on the equivalent electrical circuit [10] is used to numerically simulate the motor current signal.

As is well known, broken rotor bars in an induction machine can be detected by the presence of sideband frequencies in the stator current spectrum (Fig. 1).

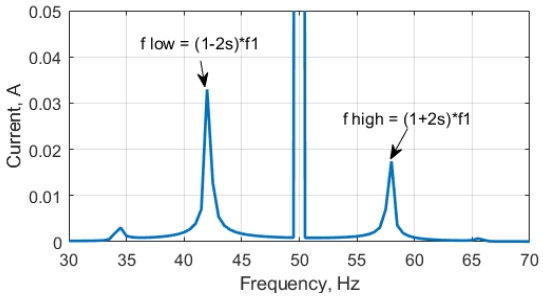

Fig. 1. Typical current spectrum for a motor with broken bars

The amplitudes of $f_{low} = (1-2s)f_1$, $f_{high} = (1+2s)f_1$ depend on fault severity and loads. Here f_1 is the supply frequency and s is the motor slip.

The impact of rotor bar faults can be modelled by unbalancing the rotor resistance [10]. A broken rotor bar is simulated by replacing the resistance of one phase of the rotor $\boldsymbol{r_r'}$ with the following value:

$$\Delta r_r' = r_r' \left(1 + \frac{3n_{bb}}{N_b - 3n_{bb}}\right),$$

where N_b is the total number of rotor bars, n_{bb} is the number of broken rotor bars.

Thus, by changing the resistance value $\Delta r_r'$ according to a linear law, it is possible to simulate the gradual degradation of the rotor bar fault from a healthy state to a complete break.

An induction four-pole motor with a power of 60 W and a supply frequency of 400 Hz was chosen as an object for modeling. This motor has a rotor with 10 bars per winding. Nominal parameters of the motor are given in Table 1.

Table 1. Nominal parameters of the motor

Nominal power P, kW	0,06
Supply voltage U_1, V	200
Field frequency, n_1, rpm	12000
Rotor speed, n, rpm	10800
Efficiency, η, %	59
Power factor, $cos\varphi$	0,56
Ratio of starting torque to nominal torque, m_s	1,81
Ratio of maximum torque to nominal torque, m_{max}	2,44
Ratio of starting current to nominal current, k_i	4,22
Nominal slip, s_r, %	10
Critical slip, s_{max}, %	46,7
Moment of inertia, J, N*m	0,0000055

The parameters of the motor model are calculated according to the method in [10] and are given in Table 2.

Table 2. Motor simulation parameters

Stator resistance, R_s, Ohm	41,1091
Rotor resistance, R_r, Ohm	8,2075
Stator inductance, L_{sp}, H	0,0051
Rotor inductance, L_{rp}, H	0,0051
Mutual inductance, L_m, H	0,1007

The motor power supply is sinusoidal. The simulation was carried out in the Simulink environment, the sampling frequency was 50 kHz.

III. THE PROPOSED METHOD

Figure 2 shows the flowchart of the proposed method which is based on the Matrix Pencil Method (MPM) [11].

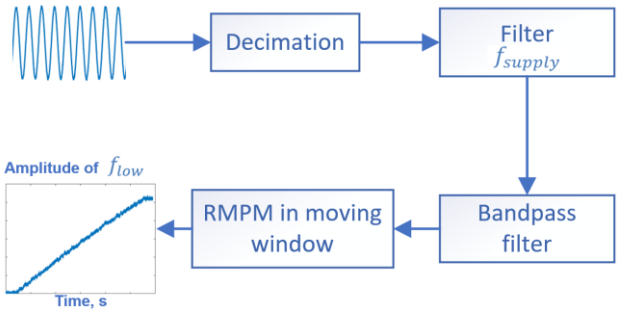

Fig. 2. Flowchart of the method

First of all, the signal is subjected to decimation, since MPM and similar methods, for example, the Prony method, work faster and more accurately when the sampling frequency does not differ significantly from the

frequencies of signal components [12]. In our example with the supply frequency of 400 Hz, the sampling rate was downsampled to 2 kHz.

At the next stage, the supply frequency is filtered. For this we use the procedure of filtering known frequency components described in Section IV.

Next, we use a conventional bandpass filter with a passband frequency range around the frequency of interest to us, usually the frequency f_{low}, the amplitude of which is greater than the amplitude of the frequency f_{high}.

For the signal that has passed such preprocessing, we use the Matrix Pencil Method. This allows us to estimate signal parameters

$$y(t) = \sum_{k=1}^{M} R_k e^{(\alpha_k + i\omega_k)t}, \quad (1)$$

from its samples

$$y(nT) = \sum_{k=1}^{M} R_k e^{(\alpha_k + i\omega_k)nT} = \sum_{k=1}^{M} R_k z_k^n, \quad (2)$$

where T is the sampling period, $R_k = A_k e^{i\varphi_k}$ are the complex amplitudes, α_k are the damping factors, $\omega_k = 2\pi f_k$ are the frequencies and $z_k = e^{(\alpha_k + i\omega_k)T}$ are the poles of $y(t)$. MPM finds the amplitudes R_k and poles z_k from samples $y(nT) = y_n$, $n = 0,1, \dots, N-1$, in two steps.

Firstly, the poles $z_k = e^{(\alpha_k + i\omega_k)T}$ can be found [9] as the generalized eigenvalues of the matrix pencil $Y_2 - \lambda Y_1$. The z_k are M eigenvalues of $Y_1^{\dagger} Y_2$, where † denotes the pseudoinverse or Moore-Penrose inverse and Y_1, Y_2 are defined as follows:

$$Y_1 = \begin{pmatrix} y_{L-1} & \cdots & y_1 & y_0 \\ y_L & \cdots & y_2 & y_1 \\ \vdots & \ddots & \vdots & \vdots \\ y_{N-3} & \cdots & y_{N-L} & y_{N-L-1} \end{pmatrix}, \quad (3)$$

$$Y_2 = \begin{pmatrix} y_L & \cdots & y_2 & y_1 \\ y_{L+1} & \cdots & y_3 & y_2 \\ \vdots & \ddots & \vdots & \vdots \\ y_{N-1} & \cdots & y_{N-L+1} & y_{N-L} \end{pmatrix}, \quad (4)$$

where $M \le L \le N - M$ is the pencil parameter. It has been shown [9] that $\frac{N}{3}$ and $\frac{2N}{3}$ are the best choices for L to ensure MPM is least sensitive to noise.

For noisy data, the Singular Value Decomposition (SVD) is used to reduce the noise and to estimate the number M of the signal poles. The SVD of the matrix Y_1 is given by:

$$Y_1 = USV^T. \quad (5)$$

Here U and V are unitary matrices and S is the diagonal matrix containing the singular values of Y_1. The superscript T notes the transpose. When arranged by magnitude, the singular values after the first M are typically very close to zero. The order M is thus estimated and the pseudoinverse $Y_1^{\dagger}$ is replaced by the rank- M truncated pseudoinverse:

$$Y_1^{\dagger} = \sum_{m=1}^{M} \frac{1}{\sigma_m} v_m u_m^T = V_0 S_0^{-1} U_0^T, \quad (6)$$

where $\sigma_1, \dots, \sigma_M$ are the M largest singular values of the matrix Y_1, v_m and u_m are the corresponding singular vectors, $V_0 = (v_0, \dots, v_M), U_0 = (u_0, \dots, u_M)$, $S_0 = diag(\sigma_1, \dots, \sigma_M)$.

The estimates of z_k can be found by computing the eigenvalues of the $M \times M$ nonsymmetrical matrix:

$$Z_E = S_0^{-1} U_0^T Y_2 V_0. \quad (7)$$

Secondly, MPM uses known M and z_k values to estiamate complex amplitudes R_k by solving the following least squares problem:

$$\begin{pmatrix} y_0 \\ y_1 \\ \vdots \\ y_{N-1} \end{pmatrix} = \begin{pmatrix} 1 & 1 & \cdots & 1 \\ z_1 & z_2 & \cdots & z_M \\ \vdots & \vdots & \ddots & \vdots \\ z_1^{N-1} & z_2^{N-1} & \cdots & z_M^{N-1} \end{pmatrix} \begin{pmatrix} R_1 \\ R_2 \\ \vdots \\ R_M \end{pmatrix} \quad (8)$$

We have set out the classical MPM which can be summarized as follows:

Algorithm 1. Classical Matrix Pencil Algorithm
Input: Signal samples

$$y_n = \sum_{k=1}^{M} R_k e^{(\alpha_k + i\omega_k)t} = \sum_{k=1}^{M} R_k z_k^n, \ n = 0,1. \dots, N-1.$$

Output: $R_k, z_k, k = 1, \dots, M$.
Start
1. Form matrices Y_1, Y_2, as in (3), (4).
2. Carry out the SVD of the matrix Y_1 (5).
3. Estimate the number M of signal poles.
4. Find the rank-M truncated pseudoinverse $Y_1^{\dagger}$ (6).
5. Find z_k by computing the eigenvalues of Z_E (7).
6. Estimate R_k by solving (8).
End

The most computationally expensive step of MPM is to calculate the SVD of the matrix composed from the signal samples. For tracking signal parameters in a moving window, when a new data point enters the data window, this matrix changes only slightly, thus, it is reasonable to find its SVD not directly but using a low-rank SVD modification procedure [13] and the SVD of the old matrix. This leads to a significant reduction in the operation time. This idea is implemented in Recursive Matrix Pencil Method (RMPM) [14] the algorithm of which we will present further.

Denote the matrices Y_1, Y_2 (3), (4) formed using the signal samples $y_0, y_1, \dots, y_{N-1}$, as $Y_1^{(0)}, Y_2^{(0)}$. Once the new data point y_N enters the data window, the older sample y_0 should be deleted. Therefore, the new matrices $Y_1^{(1)}, Y_2^{(1)}$ become

$$Y_1^{(1)} = \begin{pmatrix} y_L & \cdots & y_2 & y_1 \\ y_{L+1} & \cdots & y_3 & y_2 \\ \vdots & \ddots & \vdots & \vdots \\ y_{N-1} & \cdots & y_{N-L+1} & y_{N-L} \end{pmatrix}, \quad (9)$$

$$Y_2^{(1)} = \begin{pmatrix} y_{L+1} & \cdots & y_3 & y_2 \\ y_{L+2} & \cdots & y_4 & y_3 \\ \vdots & \ddots & \vdots & \vdots \\ y_N & \cdots & y_{N-L+2} & y_{N-L+1} \end{pmatrix}. \quad (10)$$

Having a known M-truncated SVD of $Y_1^{(0)}$, we intend to find an M-truncated SVD of $Y_1^{(1)}$. It can be realized by the procedure of low rank SVD modification method [13] and this is the important SVD step of RMPM:

Algorithm 2. Effective SVD step of RMPM

Input: M-truncated SVD of $Y_1^{(0)}$.

Output: M-truncated SVD of $Y_1^{(1)}$.

Start

1. Find SVD factors of $\begin{pmatrix} 0 & Y_1^{(0)} \end{pmatrix}$ using the known M-truncated SVD of $Y_1^{(0)} = U_0 S_0 V_0^T$ and the equality $\begin{pmatrix} 0 & Y_1^{(0)} \end{pmatrix} = USV^T = U_0(S_0 \quad 0)\begin{pmatrix} 0 & V_0^T \\ I & 0 \end{pmatrix}$.

2. Find orthogonal bases P, Q of the column spaces $(I - UU^T)A$, $(I - VV^T)B$, respectively, and set $R_A = P^T(I - UU^T)A$, $R_B = Q^T(I - VV^T)B$.

3. Construct a matrix with lower dimensions $K \in R^{(M+2)\times(M+2)}$: $K = \begin{pmatrix} I & U^TA \\ 0 & R_A \end{pmatrix}\begin{pmatrix} S & 0 \\ 0 & I \end{pmatrix}\begin{pmatrix} I & V^TB \\ 0 & R_B \end{pmatrix}$.

4. Perform the SVD on this smaller matrix $K = U_K S_K V_K^T$. Therefore, $\begin{pmatrix} Y_1^{(1)} & 0 \end{pmatrix} = (U \quad P)\, U_K\, S_K \left((V \quad Q)\, V_K\right)^T = U_1 S_K V_1^T$.

5. Obtain the desired M-truncated SVD of $Y_1^{(1)}$: $Y_1^{(1)} = U_1(:, 1{:}M) S_K(1{:}M, 1{:}M) V_1(1{:}L, 1{:}M)^T$.

End

Next algorithm describes the operation of the Recursive Matrix Pencil Method for W sets of consecutive signal segments.

Algorithm 3. Recursive Matrix Pencil Method

Input: Signal samples (W sets of N signal samples)

$$y_n = \sum_{k=1}^{M} R_k e^{(\alpha_k + i\omega_k)t} = \sum_{k=1}^{M} R_k\, z_k^n, \; n = 0,1.\ldots, N-2+W.$$

Output: $R_k,\ z_k,\ k = 1, \ldots, M$, for each set of samples $y_{w-1}, \ldots, y_{N-2+w},\ w = 1, \ldots, W$.

Start

1. Form matrix $Y_1 \equiv Y_1^{(0)}$ as in (3) from $y_0, \ldots, y_{N-1}$.

2. Carry out the SVD of the matrix Y_1.

3. Estimate the number M of signal poles.

4. Find the rank-M truncated pseudoinverse $Y_1^{\dagger}$ (6).

for $w = 1$ to W do

5. Form matrix Y_2 as in (4) from $y_{w-1}, \ldots, y_{N-2+w}$.

6. Find z_k by computing the eigenvalues of Z_E (7).

7. Estimate R_k from (8).

8. Find rank-M truncated SVD of $Y_1^{(w)}$ using **Algorithm 2.**

end

9. Form matrix Y_2 as in (4) from $y_{W-1}, \ldots, y_{N-2+W}$.

10. Find z_k by computing the eigenvalues of Z_E (7).

11. Estimate R_k from (8).

End

RMPM allows us to track the amplitude A_{low} of the harmonic f_{low} in a sliding window and notice the abnormal growth caused by the appearance of a rotor bar fault. Next, we consider an example of the proposed method.

IV. METHOD FOR FILTERING KNOWN COMPONENTS

This section proposes a method for filtering known sinusoidal components in a signal. We will use it to filter the supply frequency, the amplitude of which is hundreds of times greater than the amplitude of the sideband frequencies. This frequency represents noise interfering with the determination of side frequencies.

Let $x_n = \sum_{k=1}^{p} h_k z_k^{n-1}, n = 1, 2, \ldots$ be a signal with poles $z_k,\ k = 1, \ldots, p$. We will assume that the poles $z_1, \ldots, z_q$ are known. Our task is to obtain from the signal x_n a signal $y_n$with poles $z_{q+1}, \ldots, z_p$, which are subject to further determination, i.e., filter out known components.

The characteristic polynomial of the signal x_n is defined as follows:

$$\varphi(z) = \prod_{k=1}^{p}(z - z^k) = \sum_{m=0}^{p} a_m z^{p-m}$$

and has the following property:

$$\sum_{m=0}^{p} a_m\, x_{n-m} = \sum_{k=1}^{p} h_k z_k^{n-p-1} \sum_{m=0}^{p} a_m\, z_k^{p-m} = 0,$$

since the last factor represents the values of the characteristic polynomial at its zeros.

Let's split the characteristic polynomial of the signal x_n into known and unknown components:

$$\prod_{k=1}^{p}(z - z^k) = \prod_{k=1}^{q}(z - z^k) \cdot \prod_{k=q+1}^{p}(z - z^k)$$

$$\sum_{m=0}^{p} a_m z^{p-m} = \sum_{k=0}^{q} c_k z^{p-m} \cdot \sum_{i=0}^{p-q} \propto_i z^{p-q-i}$$

Equating coefficients at z^{p-m}, we get: $a_m = \sum_{k=0}^{q} c_k \propto_{m-k}$, where $\propto_i = 0$ for $i < 0, i > p - q$.

Substituting into equality $\sum_{m=0}^{p} a_m\, x_{n-m} = 0$ expression for the coefficients a_m, we obtain:

$$\sum_{m=0}^{p}\left(\sum_{k=0}^{q} c_k \propto_{m-k}\right) x_{n-m} = 0.$$

After some manipulations, taking into account that

$\propto_i = 0$ for $i < 0, i > p - q$, we get:

$$\sum_{m=0}^{p}\left(\sum_{k=0}^{q} c_k \propto_{m-k}\right) x_{n-m} = \sum_{m=0}^{p-q} \propto_m \sum_{k=0}^{q} c_k x_{n-m-k}.$$

Thus, $\sum_{m=0}^{p-q} \propto_m \sum_{k=0}^{q} c_k x_{n-m-k} = 0$.

Denoting $y_n = \sum_{k=0}^{q} c_k x_{n-k}$, we get

$$\sum_{m=0}^{p-q} \propto_m y_{n-m} = 0$$

Thus, y_n is the desired signal with poles $z_{q+1}, \ldots, z_p$ and a characteristic polynomial

$$\prod_{k=q+1}^{p} (z - z^k) = \sum_{i=0}^{p-q} \propto_i z^{p-q-i}.$$

To find it, we use the operation of convolution of the original signal with a sequence of c_k coefficients of the polynomial $\sum_{k=0}^{q} c_k z^{p-m} = \prod_{k=1}^{q}(z - z^k)$ with known poles.

V. RESULTS AND DISCUSSIONS

The signal considered is a 15-second model current signal with bar failure, taken with a sampling frequency of 50 kHz. The supply frequency is set to 400 Hz, as in aircraft motors. To make the example more realistic, white Gaussian noise is added to the model signal so that the signal-to-noise ratio (SNR) is about 30 dB. SNR is calculated by the formula: $SNR = 10 \lg \frac{\sum y_k^2}{\sum n_k^2}$, where y_k, and n_k are the signal and the noise samples, respectively.

Figure 3 shows the spectrum of this signal in the supply frequency region at different times. The amplitudes of the frequencies f_{low} and f_{high}, showing the presence of a bar fault, increase with time. This increase in amplitudes is what the proposed method should track.

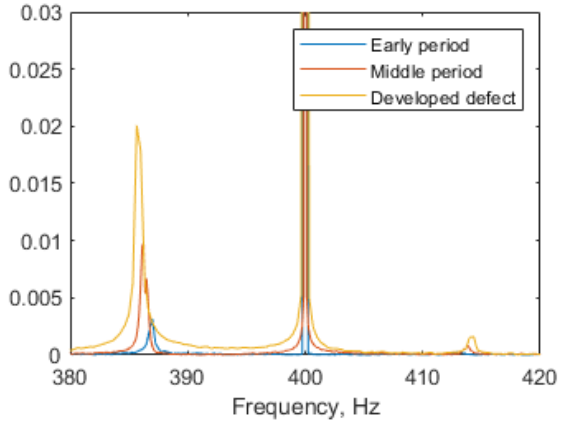

Fig. 2. Signal spectrum at different frequencies

Before proceeding to signal processing, we perform its decimation. The signal sampling frequency is 50 kHz and is too high for further signal processing by RMPM. We decimate the signal by 25 times and set the new sampling rate to 2000 Hz.

Further, we filter known frequency components from the decimated signal. Figure 4 shows the signal spectrum at different times after 400 Hz filtering. It can be seen that this frequency is absent, while the side frequencies still show an increase with time. However, the value of their amplitude decreased 10-fold compared to what was observed in the unfiltered signal (Figure 3). This is not critical, since the value of the amplitude is not important, we are tracking its behavior with the development of a defect.

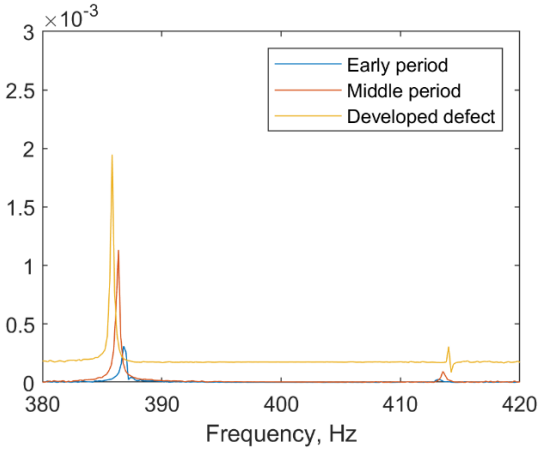

Fig. 3. Filtered signal spectrum at different frequencies

With the intention to further track the amplitude of the frequency $f_{low} \approx 386$ Hz, we apply a bandpass filter with a passband from 380 to 390 Hz. Given the length of the window, N, we track the amplitude of the frequency f_{low}. Figures 5 and 6 show the amplitude and frequency values found by the proposed method working in a moving window over the entire time interval using RMPM at $N = 100$ and 300, respectively.

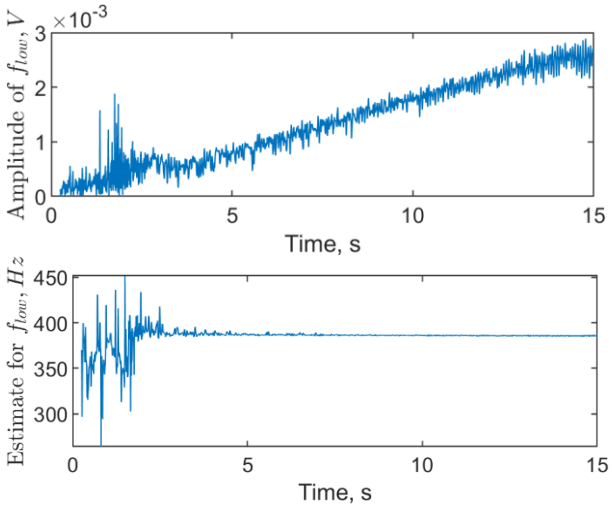

Fig. 4. Amplitude of f_{low} and f_{low} frequency at $N = 100$

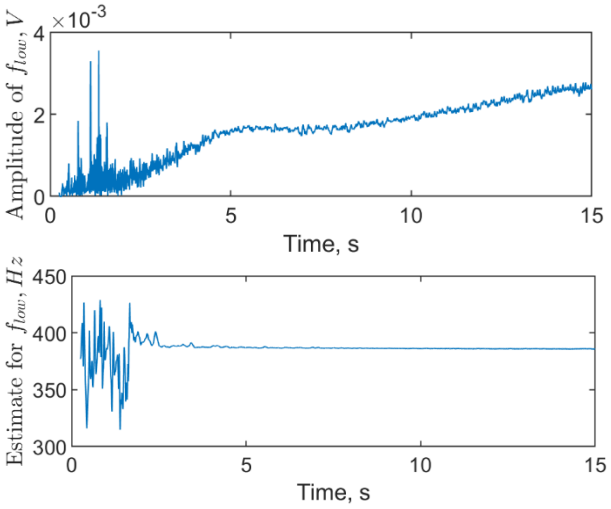

Fig. 5. Amplitude of f_{low} and f_{low} frequency at $N = 300$

It can be seen that a larger value of the window length gives a smaller variance in the parameter estimates. However, increasing the window length increases the processing time, as Table 3 shows. For comparison, the time of processing by the classical MPM is also given.

Table 3. Elapsed time

Window length, N	Time, seconds	
	RMPM	MPM
100	7	11
150	10	19
200	12	30
250	15	38
300	18	49

The time of RMPM is less than MPM, and the difference is greater at large N. With a 15-second signal, the processing time for large N can be more than 15 seconds, which indicates possible difficulties when using MPM in real time. From this point of view, the RMPM gives a significant gain in time and the possibility of practical application.

VI. CONCLUSIONS AND OUTLOOK

In this paper we have described using the Recursive Matrix Pencil Method (RMPM) for tracking the fault characteristic frequency and its amplitude in the diagnostics of induction motor rotor bar faults.

The gradual development of a bar fault was simulated, which is difficult to do experimentally. Figures 4 and 5 show that, at the initial moment – when the defect has not yet developed – the frequency and amplitude are difficult to determine. The more developed the defect, the more confidently we find a value of the frequency f_{low} and its growing amplitude A_{low}. Thus, the evaluation of the frequency and amplitude can be used as an efficient and reliable approach to diagnosing rotor bar faults.

For future work and recommendations, it is suggested to consider this analysis for DC motor diagnostic.

VII. ACKNOWLEDGMENTS

This work was financially supported by Russian Ministry of Science and Higher Education (FENU-2023-0010).

REFERENCES

[1] **Henao, H., Capolino, G.-A, et al..**: Trends in fault diagnosis for electrical machines, *IEEE Industrial electronics magazine*, Vol. 8., No. 2., 2014, pp. 31-42.

[2] **Mordor Intelligence:** Induction motor market - growth, trends, covid-19 impact, and forecasts (2022 - 2027), *https://www.mordorintelligence.com/industry-reports/induction-motor-market.* [Accessed 5th June 2023]

[3] **Garcia, M., Panagiotou, A., et al.:** Efficiency Assessment of Induction Motors Operating Under Different Faulty Conditions, *IEEE Transactions on Industrial Electronics*, Vol. 66., No. 10., 2019, pp. 8072-8081.

[4] **Singh, G.K., Sa'ad Ahmed Saleh Al Kazzaz:** Induction machine drive condition monitoring and diagnostic research – a survey, *Electric Power Systems Research*, Vol. 64., No. 2., 2003., pp. 145-158.

[5] **Kim, J. Shin, S., et al.:** Power Spectrum-Based Detection of Induction Motor Rotor Faults for Immunity to False Alarms, *IEEE Transactions on Energy Conversion*, Vol. 30., No. 3., 2015, pp. 1123–1132.

[6] **Sahraoui, M., Cardoso, A. et al.:** The Use of a Modified Prony Method to Track the Broken Rotor Bar Characteristic Frequencies and Amplitudes in Three-Phase Induction Motors, *IEEE Transactions on Industry Applications*, Vol.51, No. 3, 2015, pp. 2136–2147.

[7] **Chahine, K.:** Rotor fault diagnosis in induction motors by the matrix pencil method and support vector machine, *International Transactions on Electrical Energy Systems*, Vol. 28, No. 4, 2017.

[8] **Liu, Z., Huang, J.:** Adaptive Matrix Pencil Method for Mixed Rotor Faults Diagnosis, *2016 XXII International Conference on Electrical Machines (ICEM)*, Lausanne, Switzerland, 2016, pp. 2158–2164.

[9] **Kompella, K.C., Madhav G.V.:** Performance Analysis of Wiener Filter With Different Window Functions in Detecting Broken Rotor Fault In 3 Phase Induction Motor, *International Journal of Engineering Trends and Technology*, Vol.68, No. 12, 2020, pp. 153–159.

[10] **Chen, S., Zivanovic, R.:** Modelling and simulation of stator and rotor fault conditions in induction machines for testing fault diagnostic techniques, *European Transactions on Electrical Power*, Vol. 20., No. 5., 2010, pp. 611-629

[11] **Hua Y., Sarkar T. K.:** Matrix Pencil Method for Estimating Parameters of Exponentially Damped / Undamped Sinusoids in Noise, *IEEE Trans. Acoust.*, vol. 38, no. 5, pp. 814–824, 1990.

[12] **Bushuev O., Ibryaeva O.L.:** Choosing an Optimal Sampling Rate to Improve the Performance of Signal Analysis by Prony's Method, *35th International Conference on Telecommunications and Signal Processing (TSP)*, 2012, pp. 634–638.

[13] **Brand M.:** Fast low-rank modifications of the thin singular value decomposition, *Linear Algebra Appl.*, vol. 415, no. 1, pp. 20–30, 2006.

[14] **Ibryaeva, O.:** Recursive Matrix Pencil Method, *2nd International Ural Conference on Measurements*, 2017, 6 p.